Couette-Taylor Flow in a Dilute Polymer Solution

Alexander Groisman and Victor Steinberg
Department of Physics of Complex Systems, The Weizmann Institute of Science, 76100 Rehovot, Israel
(Received 19 April 1996)

We present experimental evidence of the striking influence of small additions of high molecular weight polymers on stability and pattern selection in Couette-Taylor flow. Two novel oscillatory flow patterns were observed. One of them is essentially due to the fluid elasticity. The other results from inertial instability modified by the elasticity. [S0031-9007(96)00915-5]

PACS numbers: 47.20.–k, 47.54.+r, 47.50.+d, 61.25.Hq

In this Letter, we report experiments showing the drastic influence of small additions of polymers on the character of instability in Couette-Taylor (CT) flow. This phenomenon has some common features with the well known drag reduction effect, when minute additions of high molecular weight polymers dramatically reduce turbulent drag. In spite of large theoretical and experimental efforts [1], the latter effect is not completely understood. The obvious difficulty here is that turbulence and rheology of polymer solutions in complex flows are both unsolved problems. The CT system is a simple arrangement of two rotating coaxial cylinders with a working fluid in the annular gap between them. In CT flow with Newtonian fluids, transition to turbulence occurs through a well known sequence of bifurcations [2]. As the rotation velocity of the inner cylinder is raised, at a particular Reynolds number Re_c the basic, purely azimuthal Couette flow bifurcates to a new, stationary, Taylor vortex flow (TVF). At a higher Re, TVF becomes wavy, and as Re grows further the flow becomes increasingly complex and chaotic. Therefore, the CT system appears to be very appropriate for the investigation of the influence of polymer additions on three-dimensional flows and flow stability.

Polymer solutions have a few properties that distinguish them from Newtonian fluids [3]. The stress field in a polymer solution is not uniquely defined by the current rate of strain, but rather depends on the flow history, with some characteristic memory time τ_r. (That is why polymer liquids are called viscoelastic.) In simple shear flow ($v_x = ky$), there is a difference between diagonal elements of the stress tensor, $N_1 = \sigma_{xx} - \sigma_{yy}$ (first normal stress difference). These two properties can provide a mechanism of energy transfer in a CT system from strong azimuthal flow in the r-θ plane to a weak vortex flow in the r-z plane (here z, r, and θ are cylindrical coordinates). A relevant parameter here is the Deborah number $\mathrm{De} = \dot{\gamma}_{\theta r}\tau_r$ (where $\dot{\gamma}_{\theta r}$ is the azimuthal shear rate), which defines the degree of stretching of the polymers. In an oscillatory flow of frequency ω, the viscoelastic force becomes increasingly out of phase with the rate of strain, as the factor $\omega\tau_r$ grows. Therefore, TVF may become oscillatory when τ_r is large enough. A point on a diagram of states, where transition lines to stationary and oscillatory vortex patterns are intersecting, is known as a codimension-two (ct) point [4]. Exploring the diagram of states in its vicinity is the main subject of this Letter.

Rheological properties of the dilute polymer solutions that we used are rather well described by the Zimm model [3], with stress given by $\boldsymbol{\sigma} = \boldsymbol{\sigma}^s + \boldsymbol{\sigma}^p$. Here, the contribution $\boldsymbol{\sigma}^s$ is due to Newtonian viscosity of the solvent, by η_s, $\boldsymbol{\sigma}^s = \eta_s\dot{\boldsymbol{\gamma}}$. The polymer part $\boldsymbol{\sigma}^p$ is, in general, flow history dependent with a whole spectrum of relaxation times. For the case of stationary flow $\boldsymbol{\sigma}^p = \eta_p\dot{\boldsymbol{\gamma}}$. So, one can introduce an apparent solution viscosity $\eta = \eta_s + \eta_p$. The polymer part of viscosity, η_p, is proportional to the polymer concentration c and viscosity of the solvent. A solution is considered as dilute, and the model is applicable, if $\eta_p < \eta_s$. A simplification of this model with a single relaxation time τ_r is given by the Oldroyd-B equation [3,5] $\boldsymbol{\sigma}^p + \tau_r\boldsymbol{\sigma}^p_{(1)} = \eta_p\dot{\boldsymbol{\gamma}}$, where $\boldsymbol{\sigma}^p_{(1)}$ is a convected time derivative. It can be derived from the molecular elastic dumbbell model [3], and proved to be rather good for describing relaxational properties and normal stress differences of dilute polymer solutions [5].

A theoretical and experimental review of instabilities in CT flow with polymer solutions has been recently given by Larson [5]. A convenient parameter of elasticity here is $\kappa = \tau_r/t_v$, where $t_v = d^2/\nu$ is the viscous diffusion time, $d = R_2 - R_1$ is the gap between the cylinders and ν is kinematic viscosity of the solution. κ does not depend on the fluid motion and is connected to De by $\mathrm{De} = \kappa\,\mathrm{Re}$. The case mainly considered was for $\eta_s = 0$ (Maxwell model). At small κ, TVF and a slight decrease of Re_c were found [6]. At large κ, oscillatory instabilities and drastic reduction of Re_c were predicted. Recent theoretical studies [7] showed that the most unstable oscillatory modes are always nonaxisymmetric, and transitions to them are probably discontinuous (backward bifurcations). A few authors [8] experimentally observed oscillatory flow patterns at Re that were close to Re_c for Newtonian liquids and presented diagrams of flow states in c-Re plane. These results are hard to interpret, though, because characterization of the solution rheology and oscillatory patterns was poor.

For our polymer solutions, we used high molecular weight PAAm [$M = (5 \div 6) \times 10^6$, with broad molecular weight distribution] and a 58% solution of saccharose

 0031-9007/96/77(8)/1480(4)$10.00

in water as a viscous solvent ($\eta_s = 42c$P s at 20 °C). A viscous solvent was required to obtain large values of κ at which the influence of elasticity on the Taylor instability becomes significant: $\tau_r \sim \eta_s$, $t_v \sim 1/\eta_s$, so $\kappa \sim \eta_s^2$.

The HAAKE 100 viscometric system that we used enabled temperature controlled measurements of viscoelastic properties of liquids in regimes of constant and oscillating shear rate. At constant shear rate, we could measure viscosity with a precision of 0.5%. Carrying out measurements in the oscillatory regime, we obtained the phase shift δ between stress and shear rate as a function of oscillation frequency ω. The solution relaxation time τ was taken as δ/ω at $\omega \to 0$ and the polymer relaxation time as $\tau_r = \tau\frac{\eta_s+\eta_p}{\eta_p}$. Oscillatory measurements at various polymer concentrations allowed us to find τ_r with a precision of about 10%. Measuring τ_r in a temperature range 10–35 °C with saccharose concentrations 50%–58%, we found good agreement with theoretically predicted $\tau_r \sim \eta_s/T$. Therefore, the relaxation time was carefully measured at a particular temperature T^0 and solvent viscosity η_s^0, and $\tau_r = \frac{\eta_s}{T}\frac{T^0}{\eta_s^0}\tau_r^0$ was substituted for other temperatures and solvent viscosities. The apparent solution viscosity η was decreasing with increasing shear rate, so we used η at $\dot{\gamma} \to 0$ for calculation of Re.

We conducted our experiments in a standard Taylor column with a stationary outer cylinder, $R_2 = 26.85$ mm, rotating inner cylinder, $R_1 = 19$ mm, and length aspect ratio $\Gamma = L/d = 54$. Temperature stability of ± 0.025 °C was achieved by circulating water in a jacket around the column. By varying the temperature in the column between 10 °C and 35 °C we could tune κ with a precision of 1% over of an order of magnitude ($\kappa \sim \eta_s^2$, $\frac{d\ln\eta_s}{dT} \simeq 0.05/°\text{C}$). Light reflecting flakes were added to solutions for flow visualization. Flow patterns were captured and digitized with the aid of a CCD camera and a frame grabber. In other experiments, the laser Doppler velocimetry (LDV) technique was used for point measurements of the axial velocity of the fluid.

Exploring flow states at different η_p/η, κ, and Re we found several novel oscillatory flow patterns, which are not observed in Newtonian fluids. The full diagram of states is described elsewhere [9,10]. Here we will concentrate on a region near the ct-point ($\kappa = \kappa_{\text{ct}}$) at which Couette flow becomes simultaneously unstable to both TVF and an oscillatory flow pattern. A typical Re-κ diagram of flow states for dilute solutions is presented in Fig. 1. One can see two new oscillatory flow states that we call rotating standing wave (RSW) and disordered oscillations (DO). Their space-time plots are shown in Figs. 2 and 3.

RSW can be viewed as a superposition of two counterpropagating waves of the same amplitude, each wave having a form of a double spiral. Such a double spiral consists of two spiral vortices spinning in opposite directions. It has a pitch of about $2d$, fills the whole column, and translationally moves through it. So, the secondary

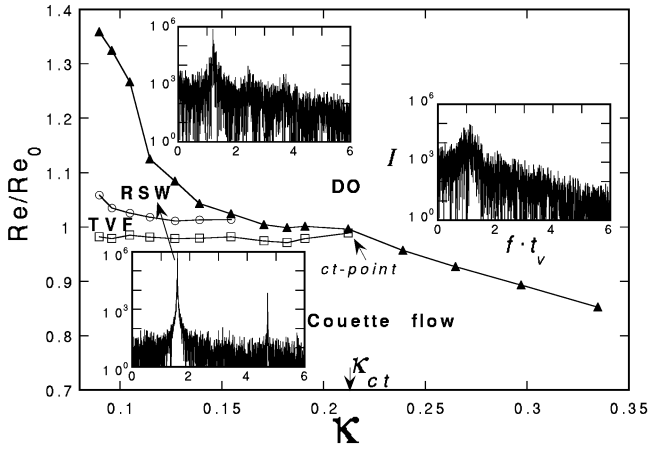

FIG. 1. Diagram of flow states for a 40 ppm solution of PAAm in 58% saccharose in water, $\eta_p/\eta_s = 0.08$. Points of transition to TVF, RSW, and DO are shown by squares, circles, and triangles, respectively. Re_0 is the Reynolds number at TVF onset in Newtonian fluids. Insets: typical frequency spectra of axial velocity for RSW, DO for $\kappa < \kappa_{\text{ct}}$, and DO for $\kappa > \kappa_{\text{ct}}$. I: intensity (arbitrary units); $f \cdot t_v$: frequency in units of the viscous diffusion time.

velocity field due to one double spiral can be generally presented as $v(\vec{r},t) = v_0(r)e^{i(\pm kz+\omega t-m\theta)}$, where "+" and "−" are for a right-handed and left-handed spiral, respectively; the azimuthal wave number m was always one. The two counterpropagating spirals always have opposite helicities, so the resulting pattern is $v_0(r)\cos(kz)e^{i(\omega t-\theta)}$. It is a standing wave in the axial direction [Fig. 2(a)] and a

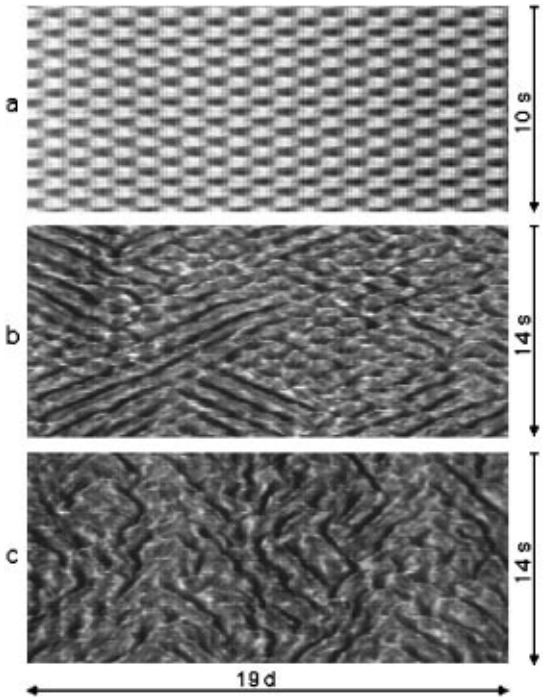

FIG. 2. Space-time plots of RSW and DO. Space coordinate is taken along the column axis. (a) RSW, (b) DO at $\kappa < \kappa_{\text{ct}}$ just above the RSW-DO transition line, and (c) DO at $\kappa > \kappa_{\text{ct}}$.

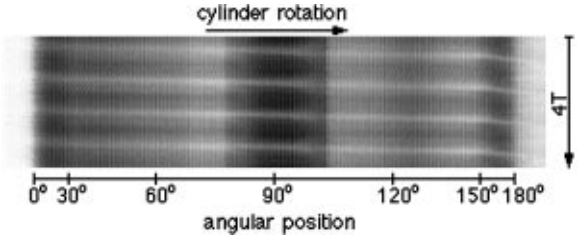

FIG. 3. Space-time plot of RSW. Space coordinate is angle around the column. T is the oscillation period. One can see a wave with $m = 1$ running in the azimuthal direction.

traveling wave in the azimuthal direction (Fig. 3). Alternatively, one can say that the pattern $v_0(r)\cos(kz)\cos\theta$ rotates around the z axis as a solid with an angular velocity ω, so that a standing wave in the axial direction is formed. The rotation direction (the sign of ω) always coincided with the direction of the inner cylinder rotation. Such a pattern was discussed in the literature [11] ("ribbons") in connection with CT flow with Newtonian fluids and counterrotating cylinders.

DO are characterized by some typical frequency, but the peaks in the frequency spectra are much broader than in the case of RSW (see insets in Fig. 1), and radial and axial velocities change in space and time rather chaotically [10]. The space-time diagram in Fig. 2(b) corresponds to a case of DO with weak disorder, where one can distinguish patches of standing and traveling waves which are randomly placed in space and time. Figure 2(c) presents DO with a stronger disorder at larger solution elasticity (insets in Fig. 1).

When the solution elasticity is low ($\kappa < \kappa_{\rm ct}$), which corresponds to small η_s and high temperature in the column, the sequence of flow patterns is the following (Fig. 1). As Re increases, first, transition to TVF occurs at Re which is lower by a few percent than Re_c for Newtonian fluids. If Re is raised further, transition to the RSW occurs, and at even higher Re, the oscillations become disordered. All these transitions are nonhysteretic. The polymer effects should disappear in the limit $\kappa \to 0$. Indeed, at sufficiently small κ, the bifurcation sequence was the same as in the Newtonian case [10].

At high solution elasticity ($\kappa > \kappa_{\rm ct}$), TVF does not appear at all, and the first instability leads to DO of a type shown in Fig. 2(c). This transition becomes increasingly hysteretic with growing κ. LDV measurements also confirm that it is a backward bifurcation [9]. Re_c significantly decreases with increasing κ. This agrees well with experimental observations of purely elastic instability at large κ and $\mathrm{Re} \to 0$ [12]. The nonaxisymmetric character of the oscillatory flow patterns and backward bifurcation to DO at large κ are also in general agreement with the recent theoretical studies [7].

Wave numbers and frequencies of oscillations are shown in Fig. 4 as functions of κ for various patterns. They were obtained from space-time diagrams using FFT and

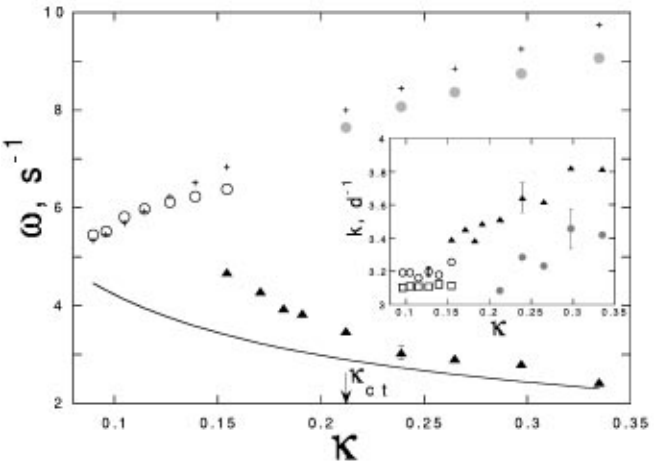

FIG. 4. Angular frequencies and wave numbers (inset) of the flow patterns from the diagram in Fig. 1 at the transition points: TVF (empty squares), RSW (empty circles), DO (full triangles), and NLO (full circles). Small crosses present 0.4Ω at the RSW and NLO onset. $1/\tau_r$ (continuous line) is shown for comparison.

autocorrelation analysis. The region $\kappa > \kappa_{\rm ct}$ is presented in Fig. 4 by two frequencies. The frequency of persistent finite amplitude DO slightly above the saddle node is shown by full triangles. One can see that this frequency roughly follows the line $1/\tau_r \sim 1/\eta_s$. We also measured the frequency of neutral linear oscillations (NLO) during transition from Couette flow to DO. They look like ordered RSW or traveling spirals. Their frequency dependence of κ is more or less a continuation of RSW frequency dependence, and it roughly follows the inner cylinder angular velocity Ω. These results suggest that we observe two different types of oscillatory modes (DO on one hand and RSW and NLO on the other) which are due to two different physical mechanisms. The wave number $k = 2\pi/\lambda$ for TVF (inset in Fig. 4) is practically the same as for Newtonian fluids ($k_c = 3.12$). The wave number of RSW is also independent of κ but about 2% larger than k_c. DO wave numbers are significantly larger than k_c and grow with κ, which is in qualitative agreement with the theoretical predictions [6,7].

The diagram of states in Fig. 1 and the value of $\kappa_{\rm ct}$ depend on η_p/η (and thus on c), which is actually the third control parameter. Exploring Re-κ diagrams at polymer concentrations up to 160 ppm, we found that the ct-point exists in a wide range of concentrations, 4.2–160 ppm, and the diagrams of states in its vicinity are similar. It is remarkable that polymer additions have a profound influence on the character of the Taylor instability even at $c = 4.2$ ppm, where the polymer contribution to the solution viscosity is only 0.8%. At higher c, when $\eta_p \simeq \eta_s$, the diagram of states changes so that a direct transition from Couette flow to RSW becomes possible [10].

The dependence of the Deborah number at the ct-point $\mathrm{De}_{\rm ct}$ on the polymer contribution to the solution viscosity

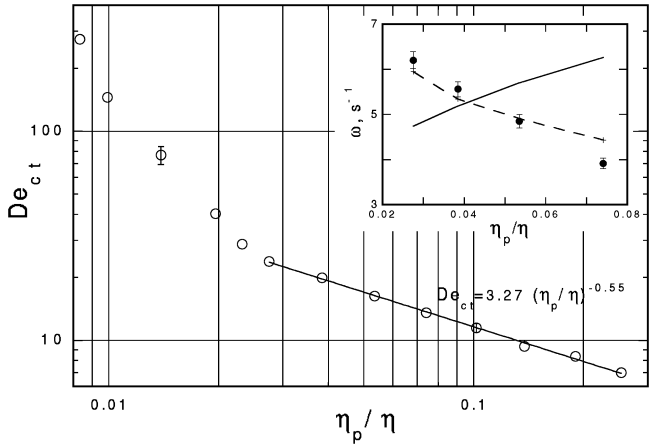

FIG. 5. De_{ct} as a function of η_p/η in the range 4.2–160 ppm of polymer concentrations. Inset: frequency ω of DO at κ_{ct} versus η_p/η. $\Omega/4$ (dashed line) and $2/\tau_r$ (continuous line) are shown for comparison.

η_p/η is shown in Fig. 5. In a rather wide range of η_p/η, from 0.028 to 0.19, which corresponds to c of 14–160 ppm, there is a good fit to a power law $De_c \sim (\eta_p/\eta)^{-0.55\pm0.01}$. This result suggests that the expression $De^2(\eta_p/\eta)$ remains almost constant at the ct-point. Since $De = \dot{\gamma}_{\theta r}\tau_r$, the polymer relaxation time τ_r and the shear rate $\dot{\gamma}_{\theta r}$ enter this expression quadratically, while η_p/η enters it only linearly. One could expect such behavior from an effect involving the first normal stress difference N_1, because $N_1 \sim \eta_p\dot{\gamma}^2$ [3].

The law $De^2(\eta_p/\eta) = \text{const}$ was actually theoretically predicted by Larson *et al.* [13], who used the Oldroyd-*B* model to consider criteria for a purely elastic instability at $Re \to 0$. The suggested mechanism was coupling of polymer elongation by weak radial flow to the strong azimuthal shear, so that the radial flow resulted in additional normal stress difference $\Delta N_1 \sim De^2\eta_p\dot{\gamma}_{rr}$. Since the system is curvilinear, $\Delta N_1/r$ acts as an additional radial pressure gradient $\Delta\frac{\partial p}{\partial r}$ (hoop stress [3]) and drives the instability. The enhancement factor De^2, which can be much larger than one, explains the way in which small additions of polymers can strongly influence the flow stability. Polymer molecules are stretched by the strong primary flow and release their large stretching energies into the weak secondary flow.

Let us now discuss the two types of oscillatory modes that we observed. DO set in at large κ and reduced Re. Their frequency is proportional to $1/\tau_r$, which is in general agreement with the predictions for the purely elastic instability [5,13]. On the other hand, parameters of RSW and NLO are rather close to those predicted for a nonaxisymmetric oscillatory mode in Newtonian fluids [14], which is purely inertial. For $R_2/R_1 = 0.708$, as in our case, the latter mode has $m = 1$, $k_c \approx 3.175$, and $\omega \approx 0.43\Omega$, but it cannot be realized in Newtonian fluids, because its critical Re is a few percent larger than Re for TVF. Thus, DO is obviously an essentially elastic mode, while RSW and NLO can be identified as an inertial mode modified by elastic effects. A detailed study of competition between these two modes will be published elsewhere [9].

This work was partially supported by the Minerva Center for Nonlinear Physics of Complex Systems.

[1] *Structure of Turbulence and Drag Reduction*, edited by A. Gyr (Springer-Verlag, Berlin, 1990).
[2] P. G. Draizin and H. Reid, *Hydrodynamic Stability* (Cambrige University Press, London, 1981).
[3] R. B. Bird, Ch. Curtiss, R. C. Armstrong, and O. Hassager, *Dynamics of Polymeric Liquids* (Wiley, New York, 1987), Vols. 1, 2.
[4] B. J. A. Zeilinska, D. Mukamel, and V. Steinberg, Phys. Rev. A **33**, 1454 (1986).
[5] R. G. Larson, Rheol. Acta **31**, 213 (1992).
[6] R. H. Thomas and K. Walters, J. Fluid Mech. **19**, 557 (1964); D. W. Beard, M. H. Davies, and K. Walters, J. Fluid Mech. **24**, 321 (1966).
[7] R. Sureshkumar, A. N. Beris, and M. Avgousti, Proc. R. Soc. London A **447**, 135 (1994).
[8] H. W. Friebe, Rheol. Acta **15**, 329 (1976); R. Haas and K. Bühler, Rheol. Acta **28**, 402 (1989).
[9] A. Groisman and V. Steinberg (to be published).
[10] A. Groisman, M.Sc. thesis, Weizmann Institute of Science, Rehovot, 1993.
[11] P. Chossat and G. Iooss, *The Couette-Taylor Problem* (Springer-Verlag, Berlin, 1994).
[12] S. J. Muller, E. S. G. Shaqfeh, and R. G. Larson, J. Non-Newton. Fluid Mech. **46**, 315 (1993); B. M. Baumert and S. J. Muller, Rheol. Acta **34**, 147 (1995).
[13] R. G. Larson, E. S. G. Shaqfeh, and S. J. Muller, J. Fluid Mech. **218**, 573 (1990); J. Non-Newton. Fluid Mech. **51**, 195 (1994).
[14] P. H. Roberts, Proc. R. Soc. London A **283**, 550 (1966).